Expanded View Figures

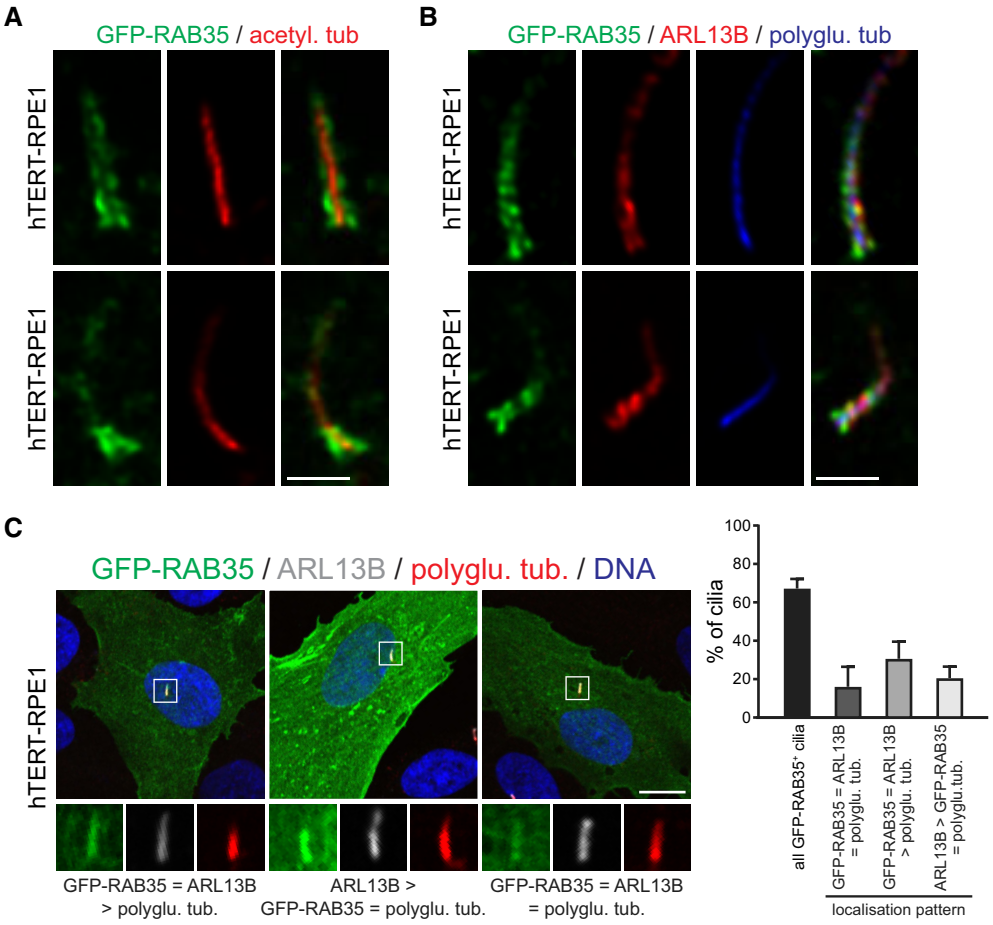

Figure EV1. Rab35 localises to the ciliary membrane.

A, B Super-resolution (FV-OSR) imaging of hTERT-RPE1 stably expressing GFP-RAB35 after 24 h serum starvation and staining for GFP and acetylated tubulin (acetyl. tub.) (A) or GFP, ARL13B and polyglutamylated tubulin (polyglu. tub.). Scale bars, 1 μm.

C Representative images of hTERT-RPE1 cells stably expressing GFP-RAB35 after 24 h serum starvation and staining for GFP, ARL13B, polyglutamylated tubulin (polyglu. tub.) and DNA. Higher magnification images of the cilia region shown to the bottom. Scale bars, 10 μm. Graph to the right shows quantification of cilia with GFP-RAB35 localisation to the proximal region of the cilium marked with polyglutamylated tubulin staining (ARL13B > GFP-RAB35 = polyglu. tub.) and cilia with GFP-RAB35 localisation along the full length of the cilium marked with ARL13B staining (ARL13B = GFP-RAB35 > polyglu. tub.). Note that in ~15% of cilia all three markers stained the same cilia region (ARL13B = GFP-RAB35 = polyglu. tub.). Data are mean ± SEM of three independent experiments ($n \geq 30$ cilia per experimental condition).

© 2019 The Authors

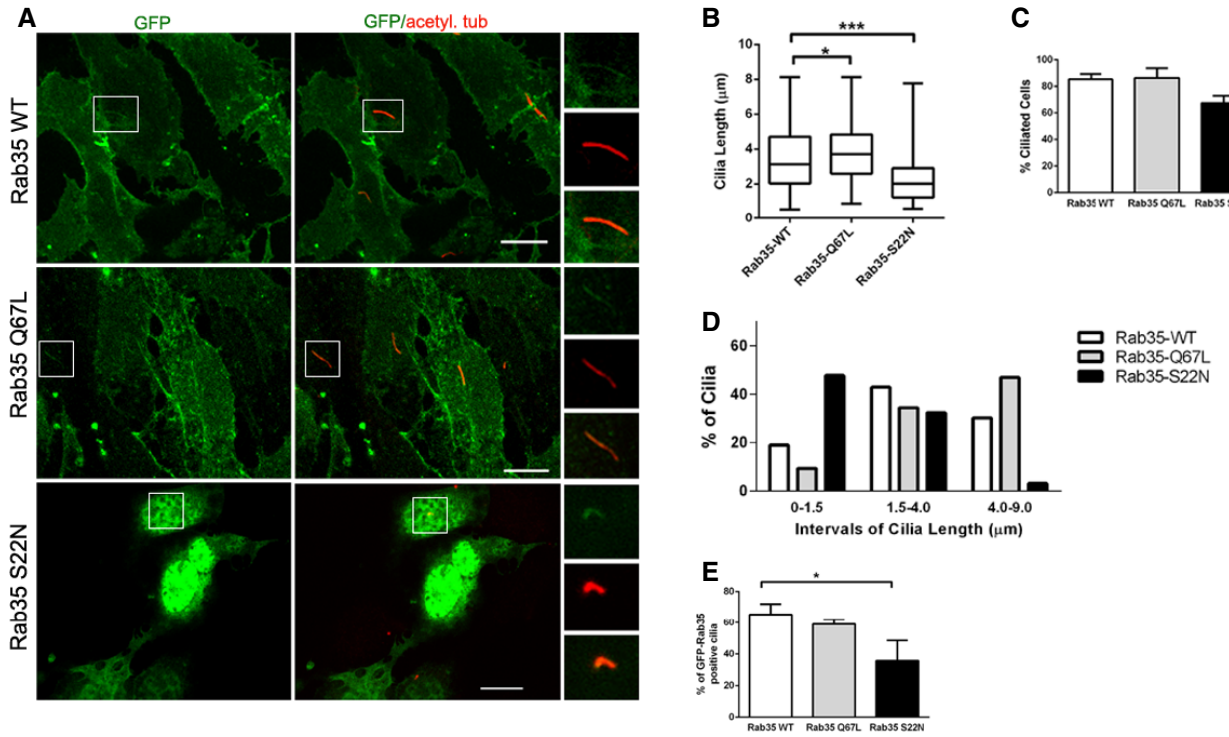

Figure EV2. Ciliary length is regulated by Rab35 nucleotide-bound state.

A Representative images of IMCD3 cells transiently expressing wild-type (WT), GDP-bound (S22N) or GTP-bound (Q67L) GFP-tagged Rab35. 12 h after transfection, cells were serum-starved for 48 h and stained for GFP and acetylated tubulin (acetyl. tub.) Higher magnification images of the cilia region shown in smaller panels. Scale bars, 10 μm.

B–E Quantification of ciliary length in μm (B), percentage of ciliation (C) and GFP-Rab35 ciliary localisation (E) in IMCD3 cells transiently expressing the indicated GFP-Rab35 constructs. Cilia length quantification in (B) is shown as box-and-whisker plots. Horizontal lines show 25, 50 and 75th percentiles; whiskers extend to minimum and maximum values. (D) Histogram of cilia length distribution in which three categories of cilia length were considered: [0–1.5 μm length]; [1.5–4 μm], and [4–9 μm]; one representative experiment out of three is shown; $n \geq 50$ cilia per experimental condition. Data in (C, E) are mean ± SEM of three independent experiments; $n \geq 100$ cilia per experimental condition. Statistical significance according to Kruskal–Wallis followed by Dunn's *post hoc* test (*$P < 0.05$, ***$P < 0.001$; Rab35-WT vs. Rab35-SN $P < 0.0001$, Rab35-WT vs. Rab35-QL $P = 0.0105$).

© 2019 The Authors

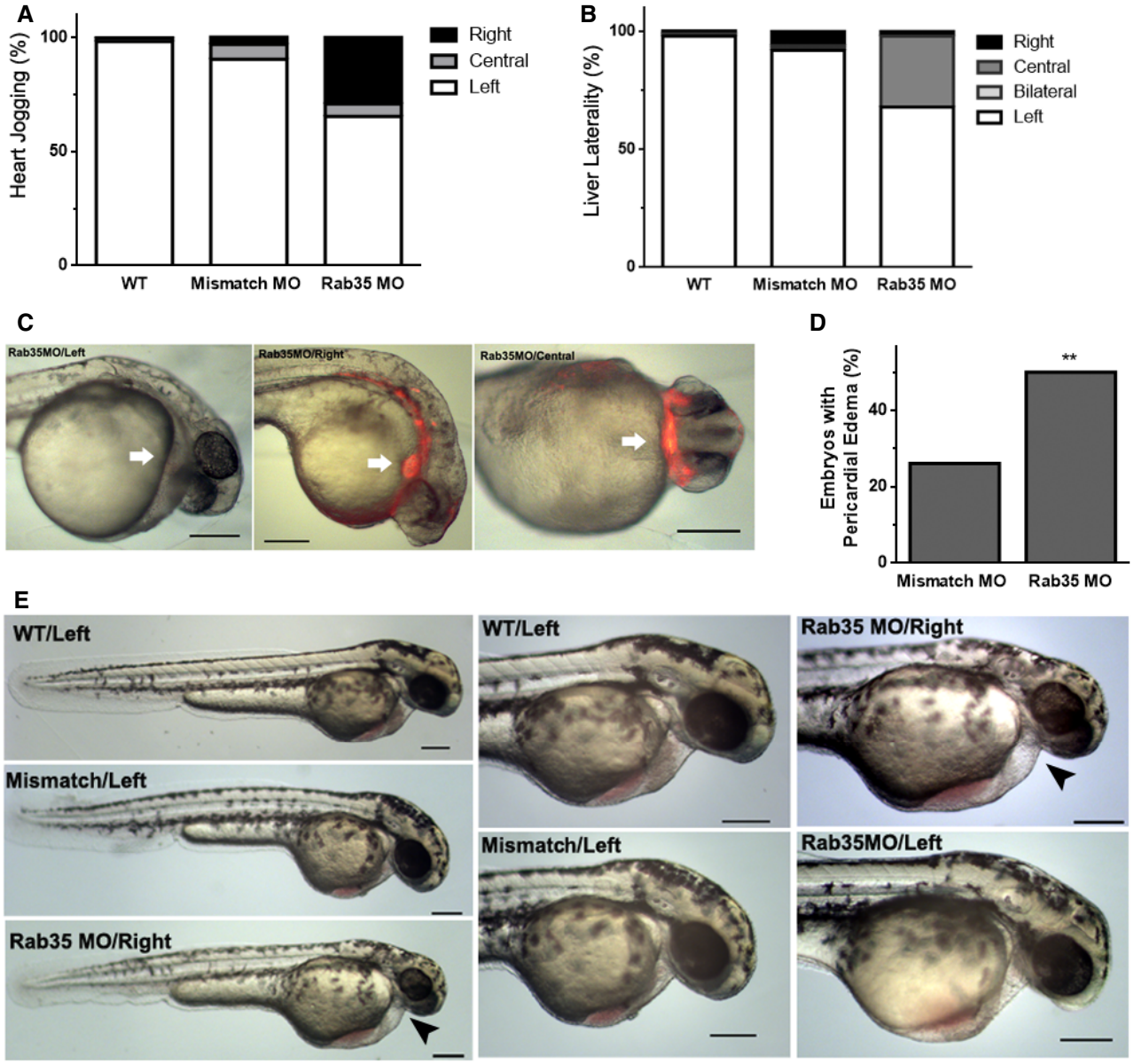

Figure EV3. Rab35 morphants present abnormal left-right patterning and pericardial oedema.

A, B Effects of Rab35 morpholino (MO) on the heart jogging and liver laterality of zebrafish embryos treated with 140 μM of MO, compared with wild-type non-injected embryos (WT) and mismatch MO, scored at 30 hpf and 53 hpf, respectively. Values are expressed as percentages (n = 3).

C Lateral or ventral view of Rab35 morphant larvae, with right-, central- or left-sided heart, at 30 hpf where heart position (red fluorescence; white arrow) is depicted as well as the absence of pericardial oedema. Scale bars, 200 μm.

D Mismatch MO control or Rab35 MO at 140 μM was injected in zebrafish embryos and pericardial oedema phenotype was quantified at 48 hpf. Statistical significance according to Fisher's exact test (**P = 0.0004; N > 20 embryos).

E Lateral view of non-injected and *Rab35* and mismatch MO morphant larvae at 48 hpf, with indication of heart positioning (left or right). Higher magnifications of lateral view are shown where the heart and pericardial oedema (when present; black arrowhead) can be appreciated. Scale bars, 200 μm.

© 2019 The Authors

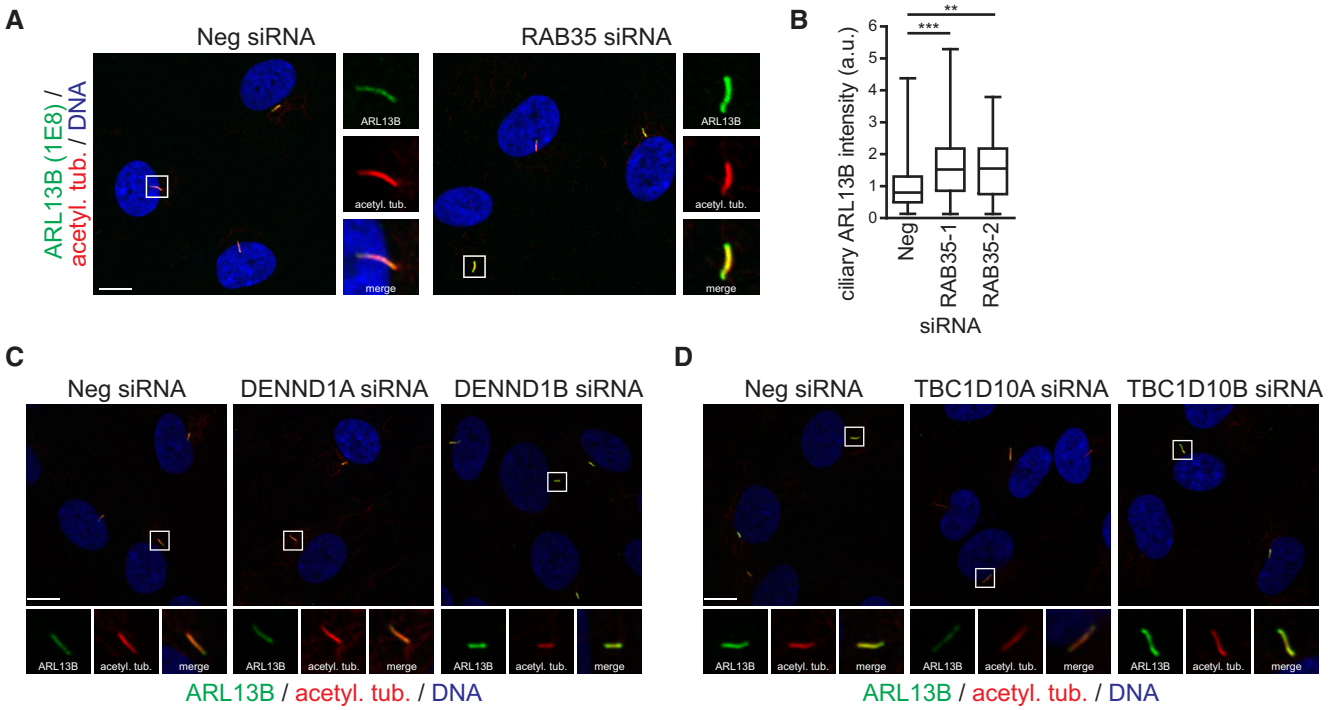

Figure EV4. RAB35, DENND1B and TBC1D10A regulate ciliary ARL13B levels in hTERT-RPE1 cells.

A, B hTERT-RPE1 cells transfected with non-targeting siRNA control (Neg) or RAB35 siRNAs were serum-starved for 48 h and stained for ARL13B (rat monoclonal antibody 1E8), acetylated tubulin (acetyl. tub.) and DNA. Representative images are shown in (A). Regions within white boxes shown at higher magnifications to the right. Scale bars, 10 μm. (B) Box-and-whisker plots show quantification of ciliary ARL13B intensity in arbitrary units (a. u.). Horizontal lines show 25, 50 and 75th percentiles; whiskers extend to minimum and maximum values. One representative experiment out of three is shown ($n > 50$ cilia per experimental condition). Statistical significance according to Kruskal–Wallis followed by Dunn's *post hoc* test (**$P < 0.01$, ***$P < 0.001$; *P*-values: Neg vs. RAB35-1 $P < 0.0017$, Neg vs. RAB35-2 $P = 0.0003$).

C, D Representative images of hTERT-RPE1 cells transfected with indicated siRNAs. Cells were serum-starved for 48 h and stained for ARL13B, acetylated tubulin (acetyl. tub.) and DNA. Regions within white boxes shown at higher magnifications in smaller panels. Scale bars, 10 μm.

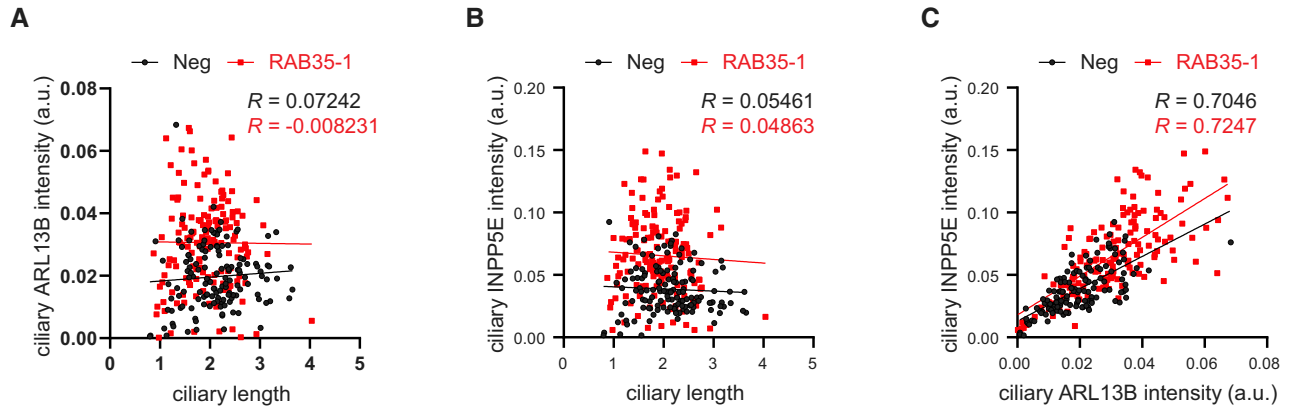

Figure EV5. Correlation analysis of ciliary length and ciliary intensity levels of ARL13B and INPP5E.

A–C hTERT-RPE1 cells transfected with non-targeting siRNA control (Neg) or RAB35 siRNA were serum-starved for 48 h and stained for ARL13B, INPP5E, acetylated tubulin and DNA. Ciliary length was measured using acetylated tubulin staining as cilia marker and mean ciliary intensities of ARL13B and INPP5E were determined. Scatterplots correlating the ciliary ARL13B levels (A) or INPP5E (B) with the ciliary length, or ciliary INPP5E levels with the ARL13B levels (C). Data points in scatterplots represent single cells (Neg: $n = 139$, Rab35-1: $n = 151$). Lines correspond to linear regressions of the data sets, with Pearson correlation coefficient *R* values indicated.

© 2019 The Authors